Collective excitations in the transitional nuclei ^{163}Re and ^{165}Re

T. R. Davis-Merry,[1] D. T. Joss,[1,*] R. D. Page,[1] J. Simpson,[2] E. S. Paul,[1] F. A. Ali,[1,†] L. Bianco,[1] R. J. Carroll,[1,‡] B. Cederwall,[3] I. G. Darby,[1,§] M. C. Drummond,[1] S. Eeckhaudt,[4] S. Ertürk,[5] M. B. Gómez-Hornillos,[2] T. Grahn,[4] P. T. Greenlees,[4] B. Hadinia,[3,‖] U. Jakobsson,[4] P. M. Jones,[4,¶] R. Julin,[4] S. Juutinen,[4] S. Ketelhut,[4,#] M. Leino,[4] P. Nieminen,[4] M. Nyman,[4] D. O'Donnell,[1,**] J. Pakarinen,[4] P. Peura,[4] P. Rahkila,[4] J. P. Revill,[1] P. Ruotsalainen,[4] M. Sandzelius,[4] P. J. Sapple,[1] J. Sarén,[4] B. Sayğı,[1] C. Scholey,[4] J. Sorri,[4] J. Thomson,[1] and J. Uusitalo[4]

[1]*Oliver Lodge Laboratory, University of Liverpool, Liverpool L69 7ZE, United Kingdom*

[2]*STFC, Daresbury Laboratory, Daresbury, Warrington WA4 4AD, United Kingdom*

[3]*Department of Physics, Royal Institute of Technology, Alba Nova Centre, S-106 91 Stockholm, Sweden*

[4]*Department of Physics, University of Jyväskylä, P.O. Box 35, FI-40014 Jyväskylä, Finland*

[5]*Nigde Universitesi, Fen-Edebiyat Falkültesi, Fizik Bölümü, Nigde, Turkey*

(Received 22 December 2014; published 17 March 2015)

Excited states in the neutron-deficient nuclei $^{163}_{75}\mathrm{Re}_{88}$ and $^{165}_{75}\mathrm{Re}_{90}$ were populated in the ^{106}Cd(^{60}Ni, $p2n\gamma$) and ^{92}Mo(^{78}Kr, $3p2n\gamma$) fusion-evaporation reactions at bombarding energies of 270 and 380 MeV, respectively. γ rays were detected at the target position using the JUROGAM spectrometer while recoiling ions were separated in-flight by the RITU gas-filled recoil separator and implanted in the GREAT spectrometer. The energy level schemes for ^{163}Re and ^{165}Re were identified using recoil-decay correlation techniques. At low spin, the yrast bands of these isotopes consist of signature partner bands based on a single $\pi h_{11/2}$ quasiproton configuration. The bands display large energy splitting consistent with the soft triaxial shape typical of transitional nuclei above $N = 82$. The configurations of the excited states are proposed within the framework of the cranked shell model.

DOI: 10.1103/PhysRevC.91.034319 PACS number(s): 23.20.Lv, 21.10.Re, 25.70.Gh, 27.70.+q

I. INTRODUCTION

The development of correlated behavior in atomic nuclei, generated by the interactions between their constituent nucleons, is an issue of central importance in nuclear physics [1,2]. Notably, the evolution of collectivity in nuclei as a function of the nucleon number is reflected in the spectrum of low-lying excited states, which vary according to the available valence space. This can be investigated as a function of neutron number in an isotopic chain. The longest chains where excited states can be identified span the $82 \leqslant N \leqslant 126$ neutron shell. For example, excited states have been identified from $^{160}_{75}$Re ($N = 85$) [3] to $^{196}_{75}$Re ($N = 121$) [4], i.e., a range of 37 nuclides.

The lightest even-N rhenium isotopes, which lie near both the $N = 82$ shell gap and the proton drip line, have ground states that are near-spherical and based on the low-Ω $s_{1/2}$ or $d_{3/2}$ proton states with a low-lying isomer formed by exciting the odd proton into the high-Ω $h_{11/2}$ state [5–9]. γ rays associated with the characteristic proton and α-particle emissions of ^{161}Re ($N = 86$) [10] have revealed excited states based on the ground state and an isomeric configuration. These noncollective excited states arise from coupling the odd proton to the few valence neutrons in $f_{7/2}$, $h_{9/2}$, and $i_{13/2}$ states.

With the addition of only a few neutrons, collective excitations become well established in ^{167}Re ($N = 92$) [11], with the observation of rotational bands. These bands are soft to triaxial deformation (γ) due to spatial density distributions of the proton and neutron orbitals at the top or bottom of their respective shells [12].

This paper discusses the structure of the neutron-deficient nuclei ^{163}Re ($N = 88$) and ^{165}Re ($N = 90$), which occupy a transitional region between noncollective and collective regimes. Prior to this work no γ-decaying excited states were known in these nuclei. The new structures identified in ^{163}Re and ^{165}Re are found to be collective and are interpreted in terms of quasiparticle configurations within the framework of the cranked shell model.

II. EXPERIMENTAL DETAILS

Excited states in ^{163}Re and ^{165}Re were populated using the reactions listed in Table I. The beam species were accelerated by the K130 cyclotron at the University of Jyväskylä Accelerator Laboratory. Prompt γ rays were detected at the target position by the JUROGAM γ-ray spectrometer [13] comprising 43 EUROGAM-type escape-suppressed HPGe detectors [14]. Recoiling fusion-evaporation residues were separated from fission products and scattered beam by the RITU gas-filled recoil separator [15,16] and deposited in

*Corresponding author: david.joss@liv.ac.uk

†Permanent address: Department of Physics, University of Sulaimani, P.O. Box 334, Sulaimani, Kurdistan Region, Iraq.

‡Present address: Department of Physics, University of Surrey, Guildford GU2 7XH, United Kingdom.

§Present address: Department of Nuclear Sciences and Applications, International Atomic Energy Agency, A-1400 Vienna, Austria.

‖Present address: Department of Physics, University of Guelph, Guelph, Ontario N1G 2W1, Canada.

¶Present address: Department of Nuclear Physics, iThemba Laboratory for Accelerator Based Sciences, P.O. Box 722, Somerset West 7129, South Africa.

#Present address: TRIUMF, 4004 Wesbrook Mall, Vancouver, British Columbia V6T 2A3, Canada.

**Present address: School of Physics and Astronomy, University of Glasgow, Glasgow G12 8QQ, United Kingdom.

TABLE I. Summary of reactions employed in the present work.

Beam species	Beam energy (MeV)	Average beam current (pnA)	Target isotope	Thickness (mg/cm^2)	Exit channel	Residual nucleus	Duration of experiment (h)
^{60}Ni	270	4	^{106}Cd	1.1	$p2n$	^{163}Re	120
^{78}Kr	380	6	^{92}Mo	0.5	$3p2n$	^{165}Re	166
^{78}Kr	357	6	^{92}Mo	1.0	$3p2n$	^{165}Re	26

the double-sided silicon strip detectors (DSSDs) of the GREAT spectrometer [17] at the separator's focal plane. All detector signals from the JUROGAM and GREAT spectrometers were passed to the total data readout acquisition system [18], where they were time stamped with a precision of 10 ns. This allows for accurate temporal correlations of γ rays detected at the target position with recoil implantations, and their subsequent radioactive decays, detected at the focal plane [19–21]. These triggerless data were sorted into $\alpha(^A\mathrm{Re})$-correlated $\gamma\gamma$ matrices and analyzed using the GRAIN [22] and RADWARE [23] analysis packages.

III. RESULTS

Figure 1(a) shows γ rays following the ^{60}Ni+^{106}Cd reaction that were detected at the target position and correlated with any recoiling nucleus detected in the DSSDs of the GREAT focal plane spectrometer. γ rays from ^{163}Re cannot be readily identified since they are swamped by the emissions from nuclei produced in other reaction channels with higher production cross sections. For example, the prominent γ rays at 288 and 433 keV originate from ^{163}Ta [24] populated via the $3p$ exit channel and the 384-, 506-, and 555-keV transitions belong to ^{163}W [25] produced in the $2pn$ reaction channel.

Previous decay-spectroscopy experiments have identified α-decay branches from both the $1/2^+$ ground state and a low-lying $11/2^-$ isomer in ^{163}Re. The α-decay properties of the $1/2^+$ ground state [$E_\alpha = 5870(5)$ keV, $t_{1/2} = 390(72)$ ms, $b_\alpha = 32(3)\%$] and $11/2^-$ isomer [$E_\alpha = 5920(5)$ keV, $t_{1/2} = 214(5)$ ms, $b_\alpha = 66(4)\%$] [26] are well suited for tagging experiments.

A total of 1.67×10^6 full-energy ($E_\alpha = 5920$ keV) $\alpha(^{163m}\mathrm{Re})$ decays were detected during the experiment. The production cross section for ^{163}Re is estimated to be 150 μb assuming a RITU separation efficiency of 50% and a 65% full-energy α-particle detection efficiency. Figure 1(b) shows a γ-ray spectrum correlated with recoils that are followed by an α decay from the $11/2^-$ isomer in ^{163}Re within the same DSSD pixel within 214 ms. This spectrum shows that the γ rays arising from the strongest reaction channels are suppressed, leaving intense γ-ray transitions at 577 and 688 keV that are not immediately apparent in the recoil-correlated spectrum. Thus, these transitions are assigned to ^{163}Re.

The energy level scheme for ^{163}Re, shown in Fig. 2, was deduced from the analysis of 2.4×10^5 $\gamma\gamma$ coincidences correlated with the α decays of ^{163}Re. The recoil-decay time correlation was limited to 214 ms to reduce false correlations with the dominant reaction channel ^{163}W, which has a longer α-decay half-life, $t_{1/2} = 2800(170)$ ms [27].

A. Excited states in ^{163}Re

Figure 3 shows γ rays in coincidence with the 577-, 688-, and 466-keV transitions. The γ-ray coincidence analysis reveals that the yrast sequence (labeled band 1) comprises signature partner bands at low spin. Figures 4(a) and 4(b) show γ rays in band 1 that are in coincidence with the 733- and 792-keV transitions. This suggests that band 1 is built upon the α-decaying $h_{11/2}$ isomer as observed in the heavier Re isotopes. Indeed, the fusion evaporation reaction used preferentially populates the high-spin $11/2^-$ and explains the nonobservation of transitions between excited states based on the $1/2^+$ ground state.

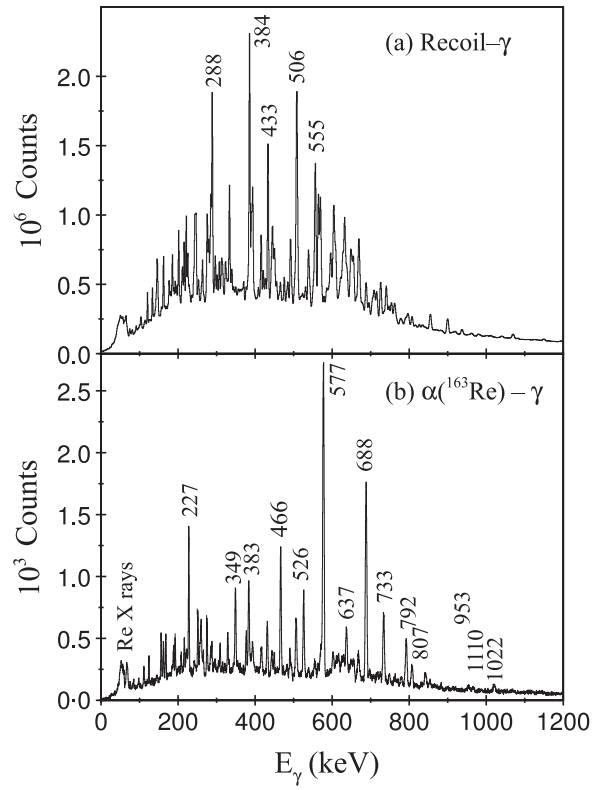

FIG. 1. (a) γ rays following the ^{60}Ni+^{106}Cd reaction and correlated with any recoil implantation detected in the GREAT DSSD located at the focal plane of the RITU separator. Prominent γ rays originating from ^{163}Ta [24] and ^{163}W [25] are labeled with their transition energies. (b) γ rays correlated with recoil implantations followed by the characteristic α decay from the $11/2^-$ isomer in ^{163}Re within the same DSSD pixel of the GREAT spectrometer. The recoil-α correlation time was limited to 214 ms.

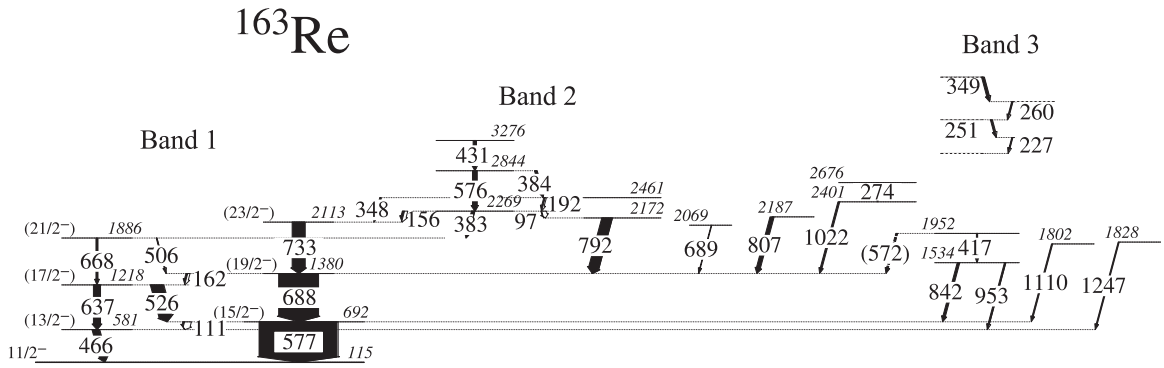

FIG. 2. Level scheme deduced for ^{163}Re. Transition and level excitation energies are given in keV and their relative intensities are proportional to the widths of the arrows. Dashed lines and parentheses indicate tentative assignments. The excitation energy of the $11/2^-$ state was measured to be 115.1(40) keV in previous work by Davids *et al.* [26].

The 192-, 384-, and 431-keV γ-ray transitions are common to these spectra and form the basis of an excited band structure (labeled band 2 in Fig. 2). Furthermore, these spectra indicate that the 733- and 156-keV transitions form a parallel decay path to the 97- and 792-keV γ rays from a common state at $E_x = 2269$ keV.

Figure 4(c) shows γ-ray coincidences with the 251-keV transition. A series of γ-ray transitions at 227, 251, 260, 275, 309, 349, and 377 keV is observed to be in coincidence with each other yet it has not been possible to place these transitions in the level scheme unambiguously. These γ rays are not in coincidence with the transitions assigned to band 2 and are therefore likely to form another band, band 3. The 227-keV γ

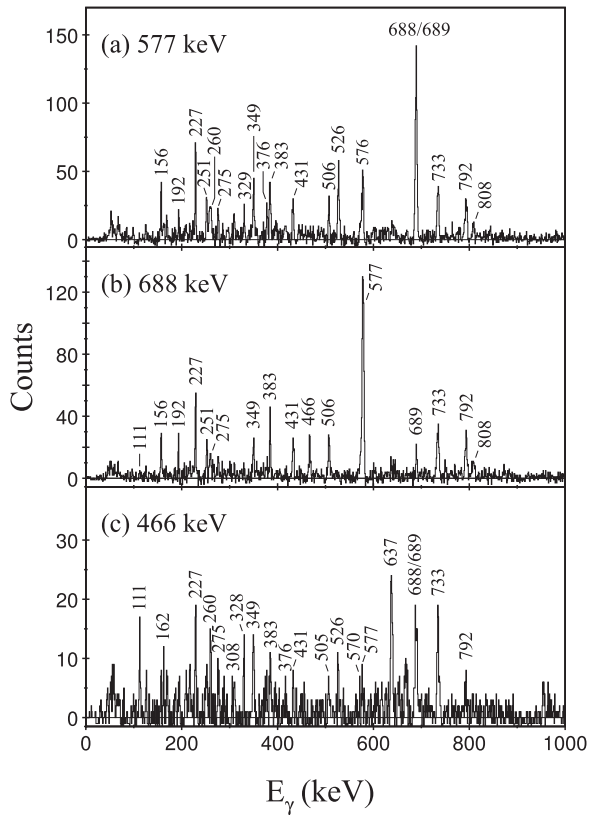

FIG. 3. γ-ray spectra extracted from a $\gamma\gamma$ coincidence matrix correlated with recoil implantations followed by the α decay from the $11/2^-$ isomer in ^{163}Re detected within the same DSSD pixel of the GREAT spectrometer. The time for recoil-decay correlations was limited to 214 ms. Spectra show coincidences with (a) the 577-keV transition, (b) the 688-keV transition, and (c) the 466-keV transition.

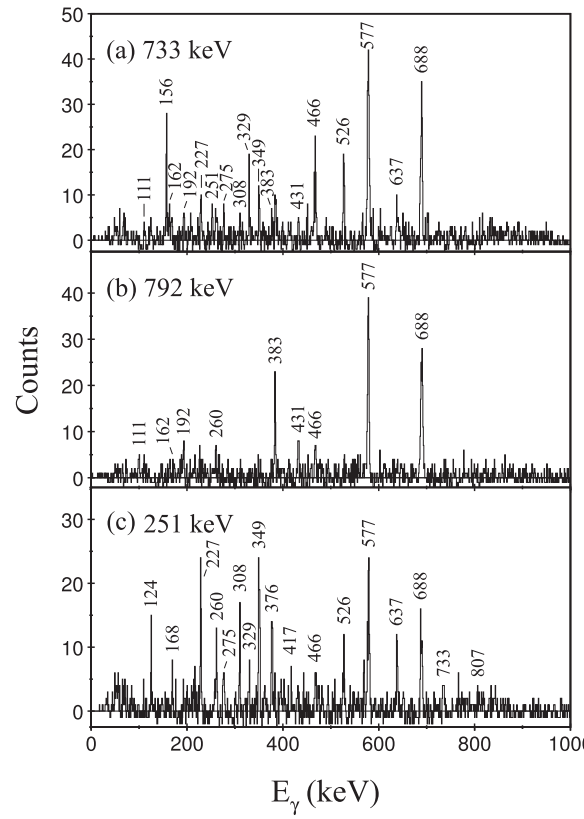

FIG. 4. γ-ray spectra extracted from a $\gamma\gamma$ coincidence matrix correlated with recoil implantations followed by the α decay from the $11/2^-$ isomer in ^{163}Re detected within the same DSSD pixel of the GREAT spectrometer. The time for recoil-decay correlations was limited to 214 ms. Spectra show coincidences with (a) the 733-keV transition, (b) the 792-keV transition, and (c) the 251-keV transition.

ray is prominent in the spectra shown in Figs. 3, 4(a), and 4(c), which suggests that this transition is placed at the bottom of band 3. The 227-keV transition feeds a state that has decay paths to the 2113-, 2187-, and 2401-keV levels but no direct linking transitions could be established.

B. Excited states in ^{165}Re

Previous decay-spectroscopy experiments have identified α-decay branches from both the $1/2^+$ ground state and a low-lying $11/2^-$ isomer in ^{165}Re [27–29]. The α-decay properties of the $1/2^+$ ground state [$E_\alpha = 5556(6)$ keV, $t_{1/2} = 1600(600)$ ms, $b_\alpha = 14(8)\%$] and $11/2^-$ isomer [$E_\alpha = 5520(6)$ keV, $t_{1/2} = 1740(60)$ ms, $b_\alpha = 13(1)\%$] [29] are not ideal for tagging experiments due to their relatively long half-lives and low branching ratios. The α (^{165m}Re) decay also overlaps the characteristic α-decay peaks from ^{166}Re [$E_\alpha = 5533(10)$ keV, $t_{1/2} = 2120(380)$ ms] [27,30,31] and ^{162}W [$E_\alpha = 5541(5)$ keV, $t_{1/2} = 1200(100)$ ms, $b_\alpha = 44(2)\%$] [27], which are produced in the fusion-evaporation reaction via the $3pn$ and $\alpha 2p2n$ exit channels, respectively. Although these nuclei have similar α-decay properties, the α decays of their daughters can easily be distinguished.

Figure 5 shows γ-ray coincidence spectra generated from recoil-decay correlations with the peak at 5520 keV detected in the GREAT DSSDs comprising the α decays of ^{165,166}Re and ^{162}W. The recoil-decay correlation time was limited to 5 s. The coincidences demanded with the 337-, 202-, and 672-keV γ rays provide evidence of a new band with strong $\Delta I = 1$ interleaving transitions. In this nucleus such a band is likely to be based on an odd-proton $h_{11/2}$ configuration. This would limit the assignment of this new band to either ^{165}Re or ^{166}Re rather than the even-even nucleus ^{162}W.

Figure 6(a) shows all α decays detected between 500 ms and 5 s after a recoil implantation within the same DSSD pixel. The minimum time difference was selected to reduce background from escaping α particles from correlated short-lived parent activities. Figure 6(b) shows all second-generation α decays preceded by the detection of a recoil implantation and a

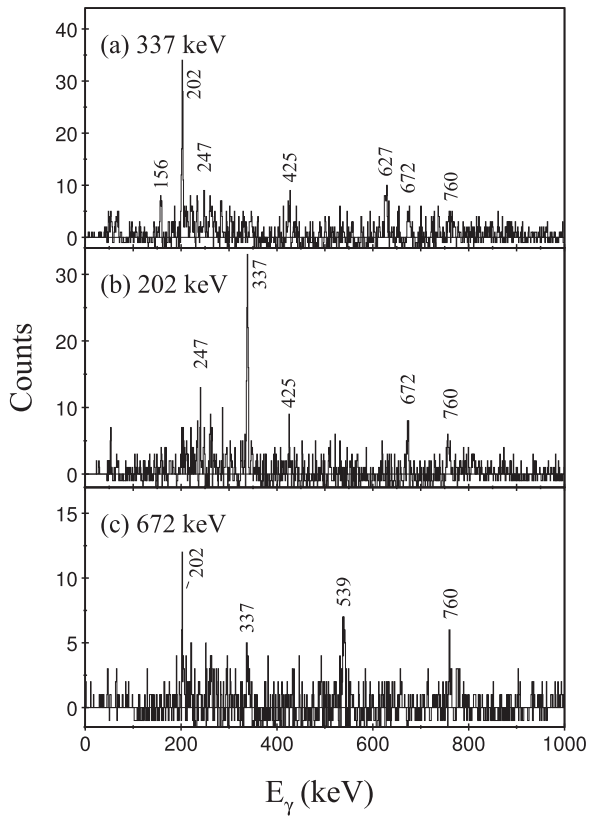

FIG. 5. γ-ray spectra extracted from a $\gamma\gamma$ coincidence matrix correlated with recoil implantations followed by the 5520-keV unresolved α decays from ^{162}W, ^{165m}Re, and ^{166}Re detected within the same DSSD pixel of the GREAT spectrometer. The time for recoil-decay correlations was limited to 5 s. Spectra show coincidences with (a) the 337-keV transition, (b) the 202-keV transition, and (c) the 672-keV transition. Transitions established in ^{165}Re (see Fig. 6) are labeled.

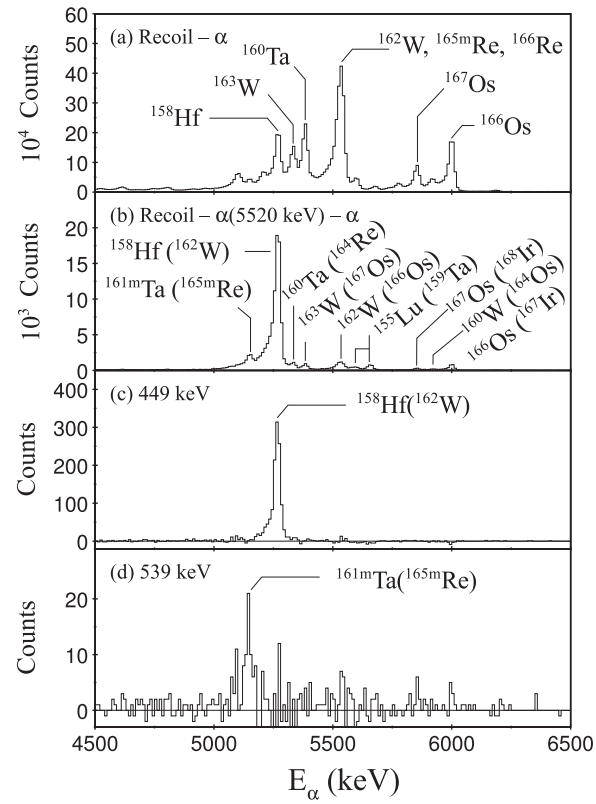

FIG. 6. Energy spectra of α particles from the ^{78}Kr+^{92}Mo reaction. (a) α particles detected between 500 and 5000 ms after a recoil implantation in the same pixel of the GREAT DSSD. (b) Second-generation α decays following a recoil implantation and the subsequent decay of the 5520-keV unresolved α-decay peaks. (c) The same conditions as for (b), with the additional constraint that the decay chain is in delayed coincidence with the 449-keV transition in ^{162}W detected at the target position. (d) The same conditions as for (b), with the additional constraint that the decay chain is in delayed coincidence with the 539-keV transition detected at the target position. The second-generation α decay of ^{161m}Ta indicates that the 539-keV γ ray is emitted by ^{165}Re.

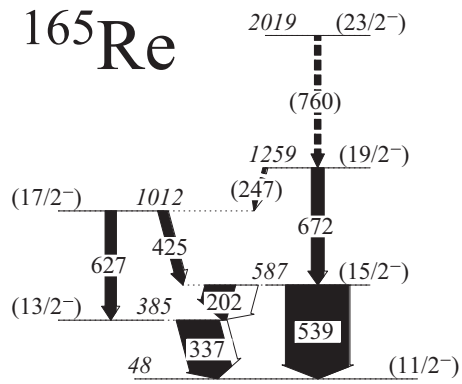

FIG. 7. Level scheme deduced for ^{165}Re from an α(5520 keV)-correlated $\gamma\gamma$ matrix. Transition energies are given in keV and their relative intensities are proportional to the widths of the arrows. Dashed lines and parentheses indicate tentative assignments. The excitation energy of the $11/2^-$ state was measured to be 48(40) keV in previous work by Poli *et al.* [34].

5520-keV α decay. The correlation time between α decays was limited to 10 s. The ^{158}Hf [27] and ^{161m}Ta [29] α-decay peaks, which originate from the ^{162}W and ^{165m}Re precursors, respectively, are prominent in the spectrum while the ^{162}Ta α decay [32] arising from the decay of ^{166}Re is not observed. There are several α-decay emissions arising from spurious decay correlations due to the long correlation time between first- and second-generation α decays. Figure 6(c) shows the second-generation α decays with the additional condition of a delayed coincidence with the 449-keV $(2^+ \rightarrow 0^+)$ γ-ray transition in ^{162}W detected at the target position [33]. An α-decay background has been subtracted to correct for correlations with the γ-ray background arising from Compton scattering. This technique is sufficiently selective to identify the second α decay in the $\alpha(^{162}\text{W}) \rightarrow \alpha(^{158}\text{Hf})$ decay chain. Similar correlations with the 539-keV γ ray, the strongest transition in the new structure, are shown in Fig. 6(d). These correlations select the $\alpha(^{165m}\text{Re}) \rightarrow \alpha(^{161m}\text{Ta})$ decay chain. The new band is therefore assigned to ^{165}Re on the basis of these correlations and the level scheme deduced from the ^{165}Re $\gamma\gamma$ coincidence analysis is shown in Fig. 7.

IV. DISCUSSION

The low-spin excited states in ^{163}Re and ^{165}Re are found to have a structure similar to that of the yrast bands in the heavier Re isotopes [11,35–38], which are based on an odd proton occupying the $h_{11/2}$ [514]9/2$^-$ Nilsson orbital. Figure 8 shows the evolution of the $9/2^-$, $13/2^-$, and $17/2^-$ ($\alpha = +1/2$) and the $15/2^-$ and $19/2^-$ ($\alpha = -1/2$) level energies relative to the $11/2^-$ state as a function of the neutron number. In ^{163}Re and ^{165}Re, the $11/2^- \rightarrow 9/2^-$ γ-ray transition is not observed. Trends in the light Re isotopes suggest that the energy difference between the $11/2^-$ state and the $9/2^-$ band head becomes very small as $N = 88$ is approached. Indeed, the measured energy difference between the $11/2^-$ and the $9/2^-$ states in ^{173}Re [39], ^{171}Re [37,38], ^{169}Re [35,36], and ^{167}Re [5] is 160, 157, 136, and 92 keV, respectively (see Fig. 8). Assuming that this trend extrapolates to ^{163}Re and that the α-decaying state has spin-parity of $9/2^-$, the transition energy between the $11/2^-$ and the $9/2^-$ states would be very low

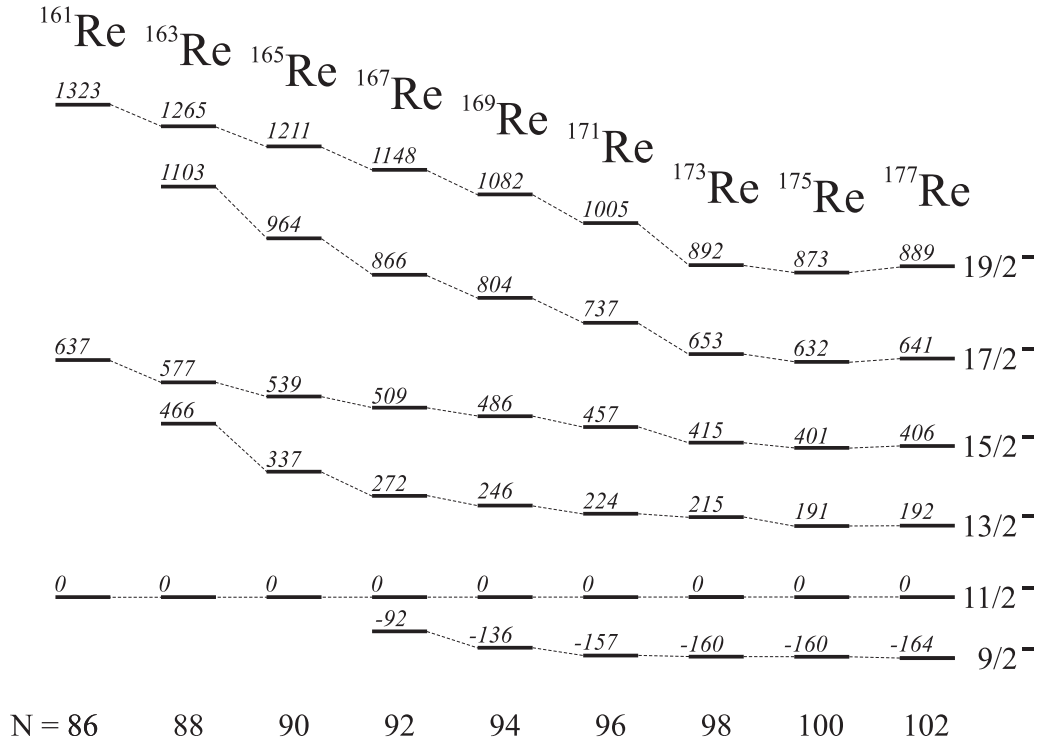

FIG. 8. Evolution of low-lying excited states in neutron-deficient transitional Re isotopes as a function of neutron number. Excitation energies of the $9/2^-$, $13/2^-$, $15/2^-$, $17/2^-$, and $19/2^-$ levels are given in keV and stated relative to the $11/2^-$ state.

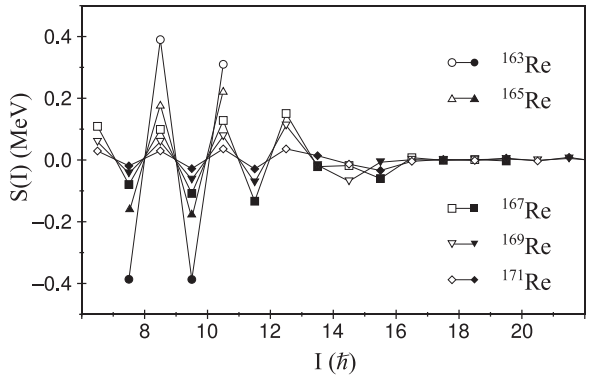

FIG. 9. Staggering parameter $S(I)$ as a function of spin I for $[514]9/2^-$ bands in the neutron-deficient odd-A rhenium isotopes ^{163}Re (band 1), ^{165}Re, ^{167}Re [11], ^{169}Re [35,36], and ^{171}Re [37,38]. Filled (open) symbols represent the $\alpha = -1/2$ ($\alpha = +1/2$) signatures, respectively.

and unlikely to be observed in the JUROGAM spectrometer. Alternatively, the $9/2^-$ state may lie above the $11/2^-$ state in ^{163}Re and ^{165}Re so that the latter is the α-decaying state. It was not possible to verify either scenario with these γ-ray data.

The level schemes of ^{163}Re and ^{165}Re have many features in common with other odd-A transitional nuclei (for example, in the Xe and Ba nuclei) [40–42]. The signature partner bands have a large degree of signature splitting at low spin, which is similar to the heavier isotope ^{167}Re [11] and the analogous structures in the odd-A Ir [43] and Ta [24,44,45] isotopes. The $\alpha = +1/2$ ($13/2^-$ and $15/2^-$) states lie near the midpoints between the levels of the opposite signature ($\alpha = -1/2$) in the isotopes near the neutron midshell at $N = 104$ (see Fig. 8), which is expected for nuclei exhibiting axial prolate symmetry. The difference in excitation energy between the $15/2^-$ and $13/2^-$ states and the $19/2^-$ and $17/2^-$ states decreases steadily below $N = 94$, showing that the degree of signature splitting increases in nuclei with closer proximity to $N = 82$.

The magnitude of the signature splitting can be highlighted by the staggering parameter $S(I)$ [46], which is defined as

$$S(I) = E(I) - E(I-1) - \tfrac{1}{2}[E(I+1) - E(I) + E(I-1) - E(I-2)]. \quad (1)$$

Figure 9 compares the staggering parameter extracted for the $h_{11/2}$ bands in ^{163}Re (band 1) and ^{165}Re with those of the heavier Re isotopes and clearly illustrates the trend of increasing signature splitting towards lower neutron numbers. The splitting is interpreted as arising from the combined core-polarizing influences of the high-Ω $h_{11/2}$ proton and the low-Ω neutron orbitals, which result in a soft triaxial shape.

The single-quasiproton configuration in the heavier isotopes $^{167-171}$Re is crossed by the three-quasiparticle $\pi h_{11/2} \otimes (\nu i_{13/2})^2$ configuration [11,35–38]. Above this crossing there is a dramatic reduction in signature splitting. This is interpreted as a change from γ-soft triaxial shapes to axially symmetric prolate deformations resulting from the rotational alignment of an $i_{13/2}$ neutron pair.

In order to speculate about the nature of three quasiparticle structures in ^{163}Re and ^{165}Re the cranked shell model has been

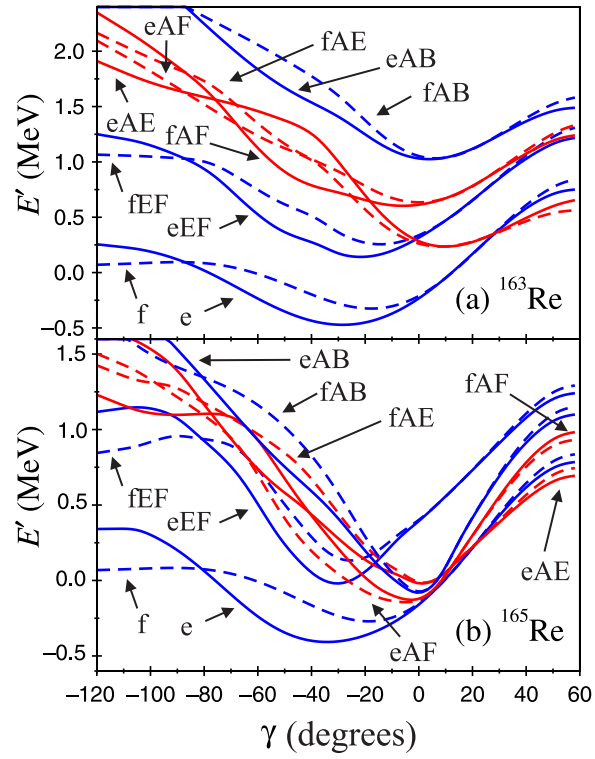

FIG. 10. (Color online) Calculated total Routhians E' as a function of γ deformation for single- and three-quasiparticle configurations in (a) ^{163}Re and (b) ^{165}Re. Routhians are calculated at a rotational frequency of 0.2 MeV and assume a prolate-oblate energy difference $V_{\rm po} = -0.4$ MeV and quadrupole deformation parameters of $\varepsilon_2 = 0.117$ and $\varepsilon_2 = 0.142$ for ^{163}Re and ^{165}Re, respectively. Deformation parameters are taken from Ref. [50]. Harris parameters are fixed at $\mathcal{J}_0 = 26\ \hbar^2\,\mathrm{MeV}^{-1}$ and $\mathcal{J}_1 = 32\ \hbar^4\,\mathrm{MeV}^{-3}$ [44]. The e, f, eEF, fEF, eAB, and fAB, configurations have negative parity [dark-gray (blue) lines], while the eAE, fAE, eAF, and fAF configurations have positive parity [light-gray (red) lines]. Solid (dashed) lines represent the $\alpha = -1/2$ ($\alpha = +1/2$) signature, respectively.

used to predict the lowest-lying configurations. The cranked shell model calculations are based on a modified Nilsson potential [47], and a γ-deformation-dependent reference is included as proposed by Frauendorf and May [48]. Total Routhians have been calculated for multiquasiparticle configurations by summing single-particle Routhians such that

$$E'(\omega,\gamma) = \sum_\mu e'_\mu(\omega,\gamma) + E'_{\rm Ref}(\omega,\gamma), \quad (2)$$

where e'_μ are the single-quasiparticle Routhians and $E'_{\rm Ref}(\omega,\gamma)$ is a γ-dependent reference defined as

$$E'_{\rm Ref}(\omega,\gamma) = \tfrac{1}{2}V_{\rm po}\cos(3\gamma) - \tfrac{3}{2}\omega^2\left(\mathcal{J}_0 + \tfrac{1}{2}\omega^2\mathcal{J}_1\right)\cos^2(\gamma + 30^\circ). \quad (3)$$

The parameter $V_{\rm po}$ is a prolate-oblate energy difference and $\mathcal{J}_0$ and $\mathcal{J}_1$ are the Harris parameters. The total Routhians for ^{163}Re and ^{165}Re are shown in Figs. 10(a) and 10(b), respectively. The labeling convention for the constituent quasiparticles from

TABLE II. Labeling convention used for single- and three-quasiparticle configurations in ^{163}Re. The convention adopted is taken from Ref. [49].

Label	Signature and parity (α, π)	Configuration
e	$(-, -1/2)$	$\pi h_{11/2}$
f	$(-, +1/2)$	$\pi h_{11/2}$
eEF	$(-, -1/2)$	$\pi h_{11/2} \otimes \nu(f_{7/2}/h_{9/2})^2$
fEF	$(-, +1/2)$	$\pi h_{11/2} \otimes \nu(f_{7/2}/h_{9/2})^2$
eAE	$(+, -1/2)$	$\pi h_{11/2} \otimes \nu[i_{13/2} \otimes (f_{7/2}/h_{9/2})]$
fAE	$(+, +1/2)$	$\pi h_{11/2} \otimes \nu[i_{13/2} \otimes (f_{7/2}/h_{9/2})]$
eAF	$(-, +1/2)$	$\pi h_{11/2} \otimes \nu[i_{13/2} \otimes (f_{7/2}/h_{9/2})]$
fAF	$(-, -1/2)$	$\pi h_{11/2} \otimes \nu[i_{13/2} \otimes (f_{7/2}/h_{9/2})]$
eAB	$(-, -1/2)$	$\pi h_{11/2} \otimes \nu(i_{13/2})^2$
fAB	$(-, +1/2)$	$\pi h_{11/2} \otimes \nu(i_{13/2})^2$

Ref. [49] is adopted and the resulting configurations are listed in Table II.

The total Routhians confirm that the lowest-energy single-quasiproton configurations are the low-spin $h_{11/2}$ bands in ^{163}Re and ^{165}Re. The single-quasiproton configurations, labeled e and f, represent the negative-parity $\alpha = -1/2$ and $\alpha = +/2$ signatures of the $h_{11/2}$ orbital, respectively. These configurations exhibit large signature splitting between the e and f Routhians in the range $-80^\circ \leqslant \gamma \leqslant -10^\circ$, which is consistent with the experimental staggering parameter obtained at low spins as shown in Fig. 9. The lowest-energy single-quasiproton Routhian (e) has a shallow minimum at $\gamma \sim -30^\circ$ corresponding to a triaxially deformed rotor.

The calculations predict that the lowest-energy three-quasiparticle structures in ^{163}Re should be negative-parity bands based on the eEF and fEF configurations. These structures are formed by coupling the odd $h_{11/2}$ proton to the mixed rotationally aligned $\nu(f_{7/2}/h_{9/2})^2$ neutron configuration. The first rotational alignment in the lighter $N = 88$ isotones ^{161}Ta [44] and ^{162}W [33] is interpreted as arising from the same EF quasineutron alignment, which is favored over the $i_{13/2}\,(AB)$ rotational alignments observed in the heavier isotopes. This is a consequence of the higher excitation energy of the $\nu i_{13/2}$ orbitals relative to the $\nu(f_{7/2}/h_{9/2})$ negative-parity states, which is attributed to the lower average deformation of the isotopes closer to the $N = 82$ shell gap. Band 2 in ^{163}Re would be a good candidate for the eEF and fEF configurations if the 192- and 384-keV transitions are the first $\Delta I = 1$ transitions between signature partner bands as indicated in Fig. 2. There are insufficient data to use signature splitting as an aid to the interpretation of this structure.

Figure 10 predicts that the prolate eAE and fAE positive-parity configurations formed by coupling the $h_{11/2}$ proton to the $i_{13/2} \otimes (f_{7/2}/h_{9/2})$ neutron orbitals are the next available three-quasiparticle configurations. Further work is needed to determine whether the transitions belonging to band 3 are based on this configuration.

The total Routhians for ^{165}Re suggest that the lowest-energy three-quasiparticle excitations should be based on configurations involving at least one $i_{13/2}$ quasineutron orbital as observed in the other $N = 90$ isotones, ^{163}Ta [24] and ^{164}W [51]. The lower excitation energy of the $i_{13/2}$ quasineutron orbital reflects the larger average deformation of ^{165}Re compared with ^{163}Re [cf. $\varepsilon_2(^{165}\text{Re}) = 0.142$, $\varepsilon_2(^{163}\text{Re}) = 0.117$) [50]. It would be interesting to extend ^{165}Re to a higher spin to investigate this prediction.

V. SUMMARY

γ-decaying excited states have been observed for the first time in the transitional nuclei ^{163}Re and ^{165}Re via precoil-decay correlations using the JUROGAM and GREAT spectrometers in conjunction with the gas-filled separator, RITU. Configuration assignments for the observed structures have been proposed based on comparisons with total Routhian calculations within the framework of the cranked shell model. Signature partner bands have been identified in both isotopes and assigned as the single-quasiproton $\pi h_{11/2}$ configuration. Candidates for the $\pi h_{11/2} \otimes \nu(f_{7/2}/h_{9/2})^2$ and the $\pi h_{11/2} \otimes \nu i_{13/2} \otimes (f_{7/2}/h_{9/2})$ three-quasiparticle configurations in ^{163}Re have been suggested on the basis of the total Routhian cranking calculations.

ACKNOWLEDGMENTS

The authors express their gratitude to the staff of the Accelerator Laboratory at the University of Jyväskylä for their excellent technical support. The authors also wish to thank Paul Morrall of the STFC Daresbury Laboratory for the preparation of the targets used in this work. Financial support for this work was provided by the UK Science and Technology Facilities Council and by the EU 6th Framework Programme, "Integrating Infrastructure Initiative—Transnational Access," Contract No. 506065 (EURONS), and by the Academy of Finland under the Finnish Centre of Excellence Programme (Nuclear and Accelerator-Based Physics Programme at JYFL). P.T.G (Grant No. 121110) and C.S. (Grant No. 209430) acknowledge the support of the Academy of Finland.

[1] A. Bohr and B. R. Mottelson, *Nuclear Structure, Vol. 1: Single-Particle Motion* (W. A. Benjamin, New York, 1969).
[2] A. Bohr and B. R. Mottelson, *Nuclear Structure, Vol. 2: Nuclear Deformation* (W. A. Benjamin, New York, 1975).
[3] P. J. Sapple *et al.*, Phys. Rev. C **84**, 054303 (2011).
[4] S. J. Steer *et al.*, Phys. Rev. C **84**, 044313 (2011).
[5] D. T. Joss *et al.*, Phys. Lett. B **641**, 34 (2006).
[6] R. D. Page *et al.*, Phys. Rev. Lett. **68**, 1287 (1992).
[7] I. G. Darby *et al.*, Phys. Rev. C **83**, 064320 (2011).
[8] I. G. Darby *et al.*, Phys. Lett. B **695**, 78 (2011).
[9] R. J. Irvine *et al.*, Phys. Rev. C **55**, R1621 (1997).
[10] K. Lagergren *et al.*, Phys. Rev. C **74**, 024316 (2006).

[11] D. T. Joss *et al.*, Phys. Rev. C **68**, 014303 (2003).
[12] Y. S. Chen, S. Frauendorf, and G. A. Leander, Phys. Rev. C **28**, 2437 (1983).
[13] C. W. Beausang and J. Simpson, J. Phys. G **22**, 527 (1996).
[14] C. W. Beausang *et al.*, Nucl. Instrum. Methods Phys. Res. A **313**, 37 (1992).
[15] J. Uusitalo *et al.*, Nucl. Instrum. Methods Phys. Res. B **204**, 638 (2003).
[16] J. Sarén, J. Uusitalo, M. Leino, and J. Sorri, Nucl. Instrum. Methods Phys. Res. A **654**, 508 (2011).
[17] R. D. Page *et al.*, Nucl. Instrum. Methods Phys. Res. B **204**, 634 (2003).
[18] I. H. Lazarus *et al.*, IEEE Trans. Nucl. Sci. **48**, 567 (2001).
[19] K.-H. Schmidt, R. S. Simon, J.-G. Keller, F. P. Hessberger, G. Münzenberg, B. Quint, H.-G. Clerc, W. Schwab, U. Gollerthan, and C.-C. Sahm, Phys. Lett. B **168**, 39 (1986).
[20] R. S. Simon, K.-H. Schmidt, F. P. Hessberger, S. Hlavac, M. Honusek, G. Münzenberg, H.-G. Clerc, U. Gollerthan and W. Schwab, Z. Phys. A **325**, 197 (1986).
[21] E. S. Paul *et al.*, Phys. Rev. C **51**, 78 (1995).
[22] P. Rahkila, Nucl. Instrum. Methods. Phys. Res. A **595**, 637 (2008).
[23] D. C. Radford, Nucl. Instrum. Methods. Phys. Res. A **361**, 297 (1995).
[24] M. Sandzelius *et al.*, Phys. Rev. C **80**, 054316 (2009).
[25] J. Thomson *et al.*, Phys. Rev. C **81**, 014307 (2010).
[26] C. N. Davids *et al.*, Phys. Rev. C **55**, 2255 (1997).
[27] R. D. Page, P. J. Woods, R. A. Cunningham, T. Davinson, N. J. Davis, A. N. James, K. Livingston, P. J. Sellin, and A. C. Shotter, Phys. Rev. C **53**, 660 (1996).
[28] C. W. Reich and R. G. Helmer, Nucl. Data Sheets **90**, 645 (2000).
[29] A. Thornthwaite *et al.*, Phys. Rev. C **86**, 064315 (2012).
[30] U. J. Schrewe, W.-D. Schmidt-Ott, R.-D. v. Dincklage, E. Georg, P. Lemmertz, H. Jungclas, and D. Hirdes, Z. Phys. A **288**, 189 (1978).
[31] F. Meissner, H. Salewski, W.-D. Schmidt-Ott, U. Bosche-Wicke, and R. Michaelsen, Z. Phys. A **343**, 283 (1992).
[32] E. Runte, T. Hild, W.-D. Schmidt-Ott, U. J. Schrewe, P. Tidemand-Petersson, and R. Michaelsen, Z. Phys. A **324**, 119 (1986).
[33] G. D. Dracoulis *et al.*, in Proceedings of the International Conference on Nuclear Structure at High Angular Momentum, Ottawa, AECL Report No. 10613, 1992, Vol. 2, p. 94.
[34] G. L. Poli *et al.*, Phys. Rev. C **59**, R2979 (1999).
[35] X. H. Zhou *et al.*, Eur. Phys. J. A **19**, 11 (2004).
[36] D. J. Hartley *et al.*, Phys. Rev. C **87**, 024315 (2013).
[37] R. A. Bark, G. D. Dracoulis, A. E. Stuchbery, A. P. Byrne, A. M. Baxter, F. Riess, and P. K. Weng, Nucl. Phys. A **501**, 157 (1989).
[38] H. Carlsson, Nucl. Phys. A **551**, 295 (1993).
[39] L. Hildingsson *et al.*, Nucl. Phys. A **513**, 394 (1990).
[40] J. Gizon and A. Gizon, Z. Phys. A **281**, 99 (1977).
[41] J. Gizon, A. Gizon, and J. Meyer-Ter-Vehn, Nucl. Phys. A **277**, 464 (1977).
[42] A. Gizon and J. Gizon, Z. Phys. A **289**, 59 (1978).
[43] M. Sandzelius *et al.*, Phys. Rev. C **75**, 054321 (2007).
[44] K. Lagergren *et al.*, Phys. Rev. C **83**, 014313 (2011).
[45] D. G. Roux *et al.*, Phys. Rev. C **63**, 024303 (2001).
[46] A. J. Kreiner, M. A. J. Mariscotti, C. Baktash, E. der Mateosian, and P. Thieberger, Phys. Rev. C **23**, 748 (1981).
[47] R. Bengtsson and S. Frauendorf, Nucl. Phys. A **327**, 139 (1979).
[48] S. Frauendorf and F. R. May, Phys. Lett. B **125**, 245 (1983).
[49] R. Wyss, J. Nyberg, A. Johnson, R. Bengtsson, and W. Nazarewicz, Phys. Lett. B **215**, 211 (1988).
[50] P. Möller, J. R. Nix, W. D. Myers, and W. J. Swiatecki, At. Data Nucl. Data Tables **59**, 185 (1995).
[51] J. Simpson, M. A. Riley, A. Alderson, M. A. Bentley, A. M. Bruce, D. M. Cullen, P. Fallon, F. Hanna, and L. Walker, J. Phys. G **17**, 511 (1991).